Enhancement of Laser Interaction with Vacuum for a Large Angular Aperture

Y. Monden[1,*] and R. Kodama[1,2]

[1]Graduate School of Engineering, Osaka University, 2-1 Yamada-oka, Suita, Osaka 565-0871, Japan

[2]Photon Pioneers Center, Osaka University, 2-1 Yamada-Oka, Suita, Osaka 565-0871, Japan

(Received 14 April 2011; published 10 August 2011)

We study the nonlinear interaction of laser light with vacuum for a large angular aperture at electromagnetic field strengths far below the Schwinger limit. The polarization and magnetization in vacuum irradiated by a focused laser beam clearly differ from those in matter. This is due to the dependence on the Lorentz invariant, which results in a ring-shaped radiation distribution in vacuum. The number of the radiated photons increases nonlinearly with increasing angular aperture.

DOI: 10.1103/PhysRevLett.107.073602 PACS numbers: 42.50.Xa, 42.65.−k

The development of ultraintense lasers [1–3] is opening up many new fields, especially in the area of high-field physics. One of the horizons in high-field physics is to generate electron-positron pairs by irradiating vacuum with visible laser light near the Schwinger limit, which is given by $I_{\text{sch}} = cE_{\text{sch}}^2/4\pi \sim 10^{29}\ \text{W/cm}^2$, where c is the speed of light and E_{sch} the field strength of the Schwinger limit [4]. Several approaches have been proposed for reducing the laser light intensity required to realize pair production [5,6]. On the other hand, a vacuum irradiated by visible laser light is expected to exhibit nonlinear optical properties at intensities far below the Schwinger limit since electron-positron pairs will be created in the vacuum for an extremely short time determined by the uncertainty principle for energy and time. Pairs with such a short lifetime will interact with a sufficient number of photons to give rise to nonlinear optical properties in vacuum. In this regime, the interaction can be treated by perturbation theory in quantum electrodynamics (QED). Wave optics is required in addition to QED when considering the optical properties in this regime. Most studies of the nonlinear optical properties in vacuum used an assumption of a small laser focusing angle (i.e., a narrow angular aperture) to simplify the complex phenomena in the vacuum [7–12]. However, advances in high energy density science and high-power laser optics are increasing the degrees of freedom of the laser focusing geometry; for example, novel focusing plasma optics with an extremely large angular aperture of over 100° has been realized that increases the focused laser intensity [13]. In addition to increasing the laser intensity, focusing a laser beam with a large angular aperture could increase the Lorentz invariants in the formula for the effective Lagrangian density of the electromagnetic field. Lorentz invariants are critical for generating polarization and magnetization in a vacuum. Thus, the small angular aperture approximation is not sufficient and more precise treatment of wave optics is required for experiments that will open up the new field of nonlinear optics in vacuum.

Here, we theoretically investigate laser interaction with a vacuum for any angular aperture by applying wave optics to QED. The polarization and magnetization in a vacuum interacted with focused laser beam increase nonlinearly with increasing angular aperture for a fixed light intensity. The radiation from the vacuum is also calculated using wave equations corrected by QED. It has a ring-shaped spatial distribution, which clearly differs from the nonlinear optical properties of matter irradiated by light. Calculations also predict that increasing the angular aperture will increase the number of radiated photons nonlinearly.

To consider the optical properties in vacuum, we use the effective Lagrangian density of the electromagnetic field presented by Heisenberg, Euler, and Schwinger [4,14]. This effective Lagrangian density $\mathcal{L}$ is valid for electromagnetic fields with wavelengths much larger than the electron Compton wavelength [15] and is represented by the sum of the conventional Lagrangian density of classical electrodynamics $\mathcal{L}_{\text{cl}}$ and the QED correction term $\mathcal{L}'$: $\mathcal{L} = \mathcal{L}_{\text{cl}} + \mathcal{L}'$. $\mathcal{L}'$ can be described in terms of the Lorentz invariants $\mathcal{F} = (|\mathbf{B}|^2 - |\mathbf{E}|^2)/2$ and $\mathcal{G} = \mathbf{E}\cdot\mathbf{B}$ of the electromagnetic field $\mathbf{E}$ and $\mathbf{B}$ by the following expansion [15,16]

$$\begin{aligned}\mathcal{L}' &= \mathcal{L}_1 + \mathcal{L}_2 + \cdots \\ &= \frac{\alpha(4\mathcal{F}^2 + 7\mathcal{G}^2)}{360\pi^2 E_{\text{sch}}^2} - \frac{\alpha\mathcal{F}(8\mathcal{F}^2 + 13\mathcal{G}^2)}{630\pi^2 E_{\text{sch}}^4} + \cdots, \end{aligned} \tag{1}$$

where $\alpha = e^2/\hbar c$ is the fine-structure constant, e the elementary charge, and $\hbar$ the reduced Planck constant. This expression is valid for field strengths below the Schwinger limit. The polarization $\mathbf{P}$ and the magnetization $\mathbf{M}$ in vacuum can be obtained using $\mathcal{L}'$ presented in Eq. (1) as follows [15]:

$$\begin{aligned}\mathbf{P} &= \frac{\partial\mathcal{L}'}{\partial\mathcal{G}}\mathbf{B} - \frac{\partial\mathcal{L}'}{\partial\mathcal{F}}\mathbf{E} = 4\xi(7\mathcal{G}\mathbf{B} - 4\mathcal{F}\mathbf{E}) + \cdots, \\ \mathbf{M} &= \frac{\partial\mathcal{L}'}{\partial\mathcal{F}}\mathbf{B} + \frac{\partial\mathcal{L}'}{\partial\mathcal{G}}\mathbf{E} = 4\xi(7\mathcal{G}\mathbf{E} + 4\mathcal{F}\mathbf{B}) + \cdots,\end{aligned} \tag{2}$$

where $\xi = \alpha/720\pi^2 E_{\text{sch}}^2$.

The representation derived from vector diffraction theory by Richards and Wolf [17] can be used to accurately consider the vector character of the electromagnetic field of the focused laser beam with a large angular aperture. According to Ref. [17], the electric and magnetic fields near the focus of the incident laser beam with a frequency ω that is linearly polarized with a homogeneous distribution on the aperture can be represented by the following forms of $\mathbf{E} = \mathrm{Re}\{\mathbf{e}e^{-i\omega t}\} = \mathbf{e}_r \cos\omega t + \mathbf{e}_i \sin\omega t$ and $\mathbf{B} = \mathrm{Re}\{\mathbf{b}e^{-i\omega t}\} = \mathbf{b}_r \cos\omega t + \mathbf{b}_i \sin\omega t$. Here, $\mathbf{e}$ and $\mathbf{b}$ are the time-independent parts of $\mathbf{E}$ and $\mathbf{B}$, respectively, Re and the subscript r denote the real part, and the subscript i denotes the imaginary part. Taking $\mathbf{E}$ and $\mathbf{B}$ to be the electromagnetic fields of the focused light, the relationship between $\mathcal{F}$ and $\mathcal{G}$ is given by $\mathcal{G}(u, v, \phi) = \mathcal{F}(u, v, \phi + \pi/4)$, where $u = kz\sin^2(\theta/2)$, $v = k\sqrt{x^2 + y^2}\sin(\theta/2)$, $k = \omega/c$, ϕ denotes the azimuthal angle in the x-y plane and θ the angular aperture. Here, the x and y axes with the origin at the focus respectively denote the directions of the electric and magnetic fields of the incident light and the z axis denotes the propagation direction of the incident light.

$\mathbf{P}$ and $\mathbf{M}$ given by Eq. (2) are expressed by $\mathbf{P} = \mathbf{P}_1 + \mathbf{P}_2 + \cdots$ and $\mathbf{M} = \mathbf{M}_1 + \mathbf{M}_2 + \cdots$, which are the sums of the polarization $\mathbf{P}_m$ and the magnetization $\mathbf{M}_m$ given by the mth term of $\mathcal{L}'$, respectively. From calculations, we obtain $\sqrt{\langle|\mathbf{P}_2|^2\rangle}_{\max}/\sqrt{\langle|\mathbf{P}_1|^2\rangle}_{\max} < 10^{-3}$ for the polarization in the vacuum irradiated by focused light with a peak intensity below 10^{27} W/cm^2, which is much lower than I_{sch}; a similar relationship holds between $\mathbf{M}_1$ and $\mathbf{M}_2$. Here, $\sqrt{\langle|\mathbf{P}_1|^2\rangle}_{\max}$ and $\sqrt{\langle|\mathbf{P}_2|^2\rangle}_{\max}$ are, respectively, the maximum values of $\sqrt{\langle|\mathbf{P}_1|^2\rangle}$ and $\sqrt{\langle|\mathbf{P}_2|^2\rangle}$ in the focal plane and the angled brackets denote the time-averaged value. In our calculations, the contributions of $\mathbf{P}_2$, $\mathbf{M}_2$, and higher components can be considered to be negligible since we consider light with peak intensities much lower than I_{sch}. Consequently, the polarization with the fundamental frequency ω in vacuum can be approximated by the lowest-order term, which leads to $\mathbf{P}$ being expressed by

$$
\begin{aligned}
\mathbf{P} \simeq\ & \xi[7\{(3\mathbf{e}_r\cdot\mathbf{b}_r + \mathbf{e}_i\cdot\mathbf{b}_i)\mathbf{b}_r + (\mathbf{e}_r\cdot\mathbf{b}_i + \mathbf{e}_i\cdot\mathbf{b}_r)\mathbf{b}_i\} \\
& + 2\{(3|\mathbf{e}_r|^2 + |\mathbf{e}_i|^2 - 3|\mathbf{b}_r|^2 - |\mathbf{b}_i|^2)\mathbf{e}_r \\
& + 2(\mathbf{e}_r\cdot\mathbf{e}_i - \mathbf{b}_r\cdot\mathbf{b}_i)\mathbf{e}_i\}]\cos\omega t \\
& + \xi[7\{(\mathbf{e}_r\cdot\mathbf{b}_i + \mathbf{e}_i\cdot\mathbf{b}_r)\mathbf{b}_r \\
& + (\mathbf{e}_r\cdot\mathbf{b}_r + 3\mathbf{e}_i\cdot\mathbf{b}_i)\mathbf{b}_i\} + 2\{2(\mathbf{e}_r\cdot\mathbf{e}_i - \mathbf{b}_r\cdot\mathbf{b}_i)\mathbf{e}_r \\
& + (|\mathbf{e}_r|^2 + 3|\mathbf{e}_i|^2 - |\mathbf{b}_r|^2 - 3|\mathbf{b}_i|^2)\mathbf{e}_i\}]\sin\omega t. \qquad (3)
\end{aligned}
$$

The magnetization $\mathbf{M}$ is similarly approximated by the lowest-order term. The relationships between the Cartesian components of these $\mathbf{P}$ and $\mathbf{M}$ are given by $M_x(u, v, \phi) = -P_y(u, v, \phi - \pi/2)$, $M_y(u, v, \phi) = P_x(u, v, \phi - \pi/2)$, and $M_z(u, v, \phi) = P_z(u, v, \phi - \pi/2)$.

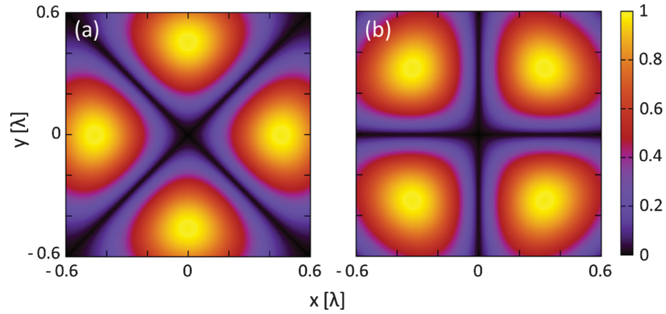

FIG. 1 (color). The distributions of the Lorentz invariants (a) $|\langle\mathcal{F}\rangle|$ and (b) $|\langle\mathcal{G}\rangle|$ of the focused laser beam in the focal plane for $\theta = 100°$. The x and y axes are expressed in units of the laser wavelength λ. The Lorentz invariants are normalized to the peak value.

We take the laser wavelength to be $\lambda = 1\ \mu$m. Figure 1 shows the spatial distributions of the Lorentz invariants $|\langle\mathcal{F}\rangle|$ and $|\langle\mathcal{G}\rangle|$ of the focused laser beam in the focal plane for $\theta = 100°$, where the x and y axes are parallel to the directions of the electric and magnetic fields of the incident laser beam, respectively. As Fig. 1(a) shows, $|\langle\mathcal{F}\rangle|$ completely vanishes at the focus but has peak values on the x and y axes. This nonzero value of $|\langle\mathcal{F}\rangle|$ originates from the fact that the distributions of the electric and magnetic field amplitudes of the focused light are not the same, but are elliptical with their major axes lying, respectively, along the x and y axes, despite the fields of the incident light having homogeneous distributions [17]. These rotationally asymmetric distributions of the fields near the focus, which arise from focusing a linearly polarized laser beam, have been studied theoretically and experimentally [17–19]. The distribution of $|\langle\mathcal{G}\rangle|$ shown in Fig. 1(b) is given by the above-mentioned relationship between the Lorentz invariants. Figures 2(a) and 2(b) show the spatial distributions of the polarization and magnetization $\mathbf{P}$ and $\mathbf{M}$ given by Eq. (3) in the focal plane for $\theta = 100°$, respectively. The

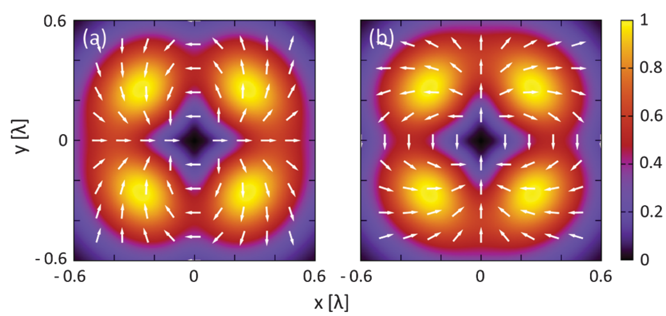

FIG. 2 (color). The distributions of the amplitudes (colors) and directions (white arrows) of (a) the polarization $\mathbf{P}$ and (b) the magnetization $\mathbf{M}$ described by Eq. (3) in the focal plane for $\theta = 100°$. The amplitudes of $\mathbf{P}$ and $\mathbf{M}$ are given by $\sqrt{\langle|\mathbf{P}|^2\rangle}$ and $\sqrt{\langle|\mathbf{M}|^2\rangle}$, respectively. The x and y axes are expressed in units of the laser wavelength λ. The amplitudes are normalized to the peak value.

colors represent $\sqrt{\langle|\mathbf{P}|^2\rangle}$ and $\sqrt{\langle|\mathbf{M}|^2\rangle}$, which correspond to the amplitudes of **P** and **M**, and the white arrows indicate their directions. The specific distributions of the amplitudes and directions of **P** and **M** are attributed to the dependences of the polarization and magnetization in vacuum on the Lorentz invariants shown in Fig. 1, which (unlike in matter) are determined by the relationship between the electric and magnetic fields.

The elliptical distributions of the amplitudes of the electric and magnetic fields become more pronounced with increasing angular aperture due to the increase in the longitudinal z components of the fields since the elliptical distributions are mainly attributed to the longitudinal components [19]. Therefore, the magnitudes of the Lorentz invariants $\mathcal{F}$ and $\mathcal{G}$ increase with increasing angular aperture, enhancing the polarization and magnetization in the vacuum. This is summarized in Fig. 3, where the maximum value of the amplitude $\sqrt{\langle|\mathbf{P}|^2\rangle}$ in the focal plane is equal to that of $\sqrt{\langle|\mathbf{M}|^2\rangle}$ and increases with increasing angular aperture for a constant laser intensity.

Next, we consider the electromagnetic field radiated from the vacuum. From the Maxwell equations including the QED correction term $\mathcal{L}'$, the wave equations in the vacuum are obtained as follows:

$$\begin{aligned}\Box\mathbf{E} &= -4\pi\left[\nabla(\nabla\cdot\mathbf{P}) - \frac{1}{c^2}\frac{\partial^2\mathbf{P}}{\partial t^2} - \frac{1}{c}\nabla\times\frac{\partial\mathbf{M}}{\partial t}\right],\\ \Box\mathbf{B} &= -4\pi\left[\frac{1}{c}\nabla\times\frac{\partial\mathbf{P}}{\partial t} + \nabla\times(\nabla\times\mathbf{M})\right],\end{aligned} \tag{4}$$

where $\Box = \nabla^2 - \partial^2/\partial(ct)^2$. The radiated electric and magnetic fields $\mathbf{E}_r$ and $\mathbf{B}_r$ are obtained by solving

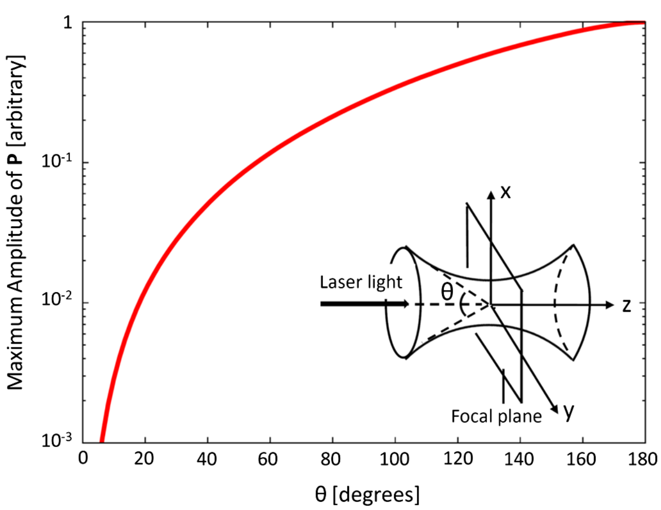

FIG. 3 (color online). Angular aperture dependence of the maximum amplitude of the polarization **P** in the focal plane under a fixed laser intensity, and geometric configuration of the incident laser light. The maximum amplitude of **P** is equal to that of the magnetization **M**. The amplitude is normalized to the value for $\theta = 180°$.

Eq. (4). In our calculations, the contributions of $\mathbf{E}_r$ and $\mathbf{B}_r$ to **P** and **M** can be neglected because these components are much smaller than the electromagnetic field of the focused light, which dominates in the generation of **P** and **M**. The number of photons radiated from the vacuum per laser shot can be defined by using $\mathbf{E}_r$ and $\mathbf{B}_r$ as follows

$$N \simeq \frac{\tau}{\hbar\omega}\int_S \left|\left\langle\frac{c}{4\pi}\mathbf{E}_r\times\mathbf{B}_r\right\rangle\right| dS, \tag{5}$$

where S is the domain of the surface integral and the laser pulse is assumed to be rectangular with a duration τ.

Figures 4(a) and 4(b), respectively, show the intensity distributions of the focused light with no interaction with vacuum and the radiated electromagnetic field with the fundamental frequency for an f number of $f/\# = 0.4$ ($\theta \simeq 103°$), where $f/\#$ is defined as focal length divided by aperture diameter. The x-y plane is located $20\lambda = 20\ \mu$m from the focal plane in the propagation direction of the incident light and each intensity is normalized by its peak value. The radiated field in Fig. 4(b) is obtained by calculating the wave equations Eq. (4) taking **P** and **M** to be the source of the radiated field. The radiated field has a ring-shaped distribution completely different from that of the focused light, and reflects the distributions of the amplitudes of **P** and **M** shown in Fig. 2.

Figure 5 shows the number of the radiated photons polarized perpendicular to the incident laser light as a function of the laser power for $\tau = 100$ fs. The solid, dashed, and dot-dashed lines indicate the calculation results for $f/\# = 0.4$, 1 ($\theta \simeq 53°$), and 4 ($\theta \simeq 14°$), respectively. In the case of $f/\# = 0.4$; i.e., $\theta \simeq 103°$, the number of the photons reaches approximately 4×10^4 for 200 PW which will be realized in the future project [2]. Comparison of the results for $\theta \simeq 103°$ and $\theta \simeq 53°$ for the same laser power reveals that the number of radiated photons

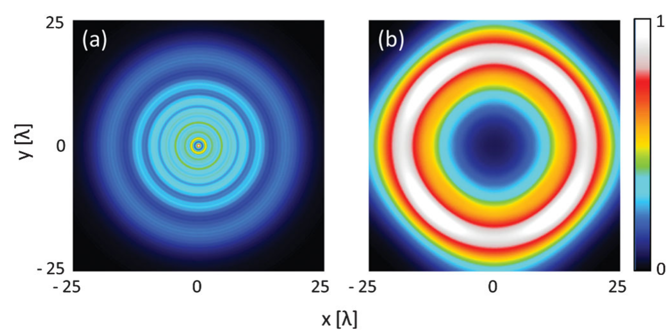

FIG. 4 (color). The intensity distributions of (a) the focused laser beam with no interaction with vacuum and (b) the electromagnetic field radiated from the vacuum irradiated by a focused beam in the plane located $20\lambda = 20\ \mu$m from the focal plane in the propagation direction of the incident laser beam. The f number is assumed to be 0.4 (i.e., $\theta \simeq 103°$). The peak intensities of the focused light and the radiated field are about 10^{22} W/cm^2 and 10^4 W/cm^2 for a laser power of 100 PW, respectively. The intensities are normalized to their peak values.

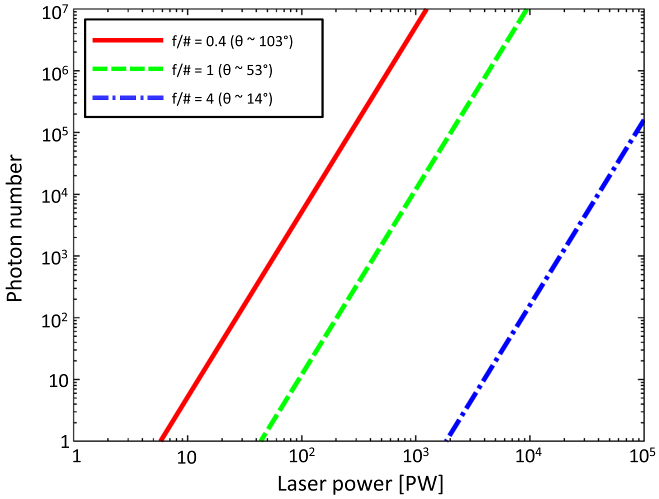

FIG. 5 (color online). The number of the radiated photons polarized perpendicular to the incident laser light per shot as a function of the laser power for $\tau = 100$ fs.

increases by 2 orders of magnitude on doubling the angular aperture. Moreover, reducing the f number from 4 to 0.4, which corresponds approximately increasing the angular aperture by a factor of 7, enhances the number of photons by 7 orders of magnitude. From Eqs. (4) and (5), the number of the radiated photons is roughly proportional to the square of the polarization and magnetization. Figure 3 shows that the polarization increases approximately by a factor of 60 through increasing the angular aperture from 14° to 103° under a fixed laser intensity. Then, the seven order enhancement of the number of photons consists of the three order enhancement (by the increases in the polarization and magnetization independent of the increase in the laser intensity) and the four order enhancement (by geometrical effects with decreasing focal spot size).

In this study, we investigated the interaction of a focused laser beam with a vacuum for a large angular aperture. We found that the number of photons radiated from a vacuum irradiated by a focused beam increases nonlinearly with increasing angular aperture; for example, the photon number is enhanced by 7 orders of magnitude when the angular aperture is increased by a factor of 7 for a fixed laser power. The radiated electromagnetic field has a ring-shaped intensity distribution and contains a component oscillating perpendicular to the polarization of the incident laser beam. This is because the polarization and magnetization in the vacuum clearly differ from those in matter due to the dependence on the Lorentz invariants. These results reveal that employing a large angular aperture will facilitate the detection of nonlinear optical properties in a vacuum.

We would like to acknowledge discussions with Dr. M. Nakatsutsumi and Dr. K. Shibata. This work was supported by the Global COE Program, "Center for Electronic Devices Innovation," and the JST-CREST program, "High Energy Density Plasma Photonics."

*ymonden@ef.eie.eng.osaka-u.ac.jp

[1] V. Yanovsky *et al.*, Opt. Express **16**, 2109 (2008).
[2] Extreme Light Infrastructure (ELI), ELI Scientific Case [http://www.extreme-light-infrastructure.eu/ELI-scientific-case_2_4.php].
[3] High Power Laser Energy Research (HiPER), Technical Background and Conceptual Design [http://www.hiper-laser.org/overview/TDR/tdr.asp].
[4] J. Schwinger, Phys. Rev. **82**, 664 (1951).
[5] N. B. Narozhny *et al.*, Phys. Lett. A **330**, 1 (2004).
[6] S. S. Bulanov *et al.*, Phys. Rev. Lett. **104**, 220404 (2010).
[7] T. Heinzl *et al.*, Opt. Commun. **267**, 318 (2006).
[8] E. Lundström *et al.*, Phys. Rev. Lett. **96**, 083602 (2006).
[9] A. M. Fedotov and N. B. Narozhny, Phys. Lett. A **362**, 1 (2007).
[10] N. B. Narozhny and A. M. Fedotov, Laser Phys. **17**, 350 (2007).
[11] A. Di Piazza, K. Z. Hatsagortsyan, and C. H. Keitel, Phys. Rev. Lett. **97**, 083603 (2006).
[12] B. King, A. Di Piazza, and C. H. Keitel, Phys. Rev. A **82**, 032114 (2010).
[13] M. Nakatsutsumi *et al.*, Opt. Lett. **35**, 2314 (2010).
[14] W. Heisenberg and H. Euler, Z. Phys. **98**, 714 (1936).
[15] V. B. Berestetskii, E. M. Lifshitz, and L. P. Pitaevskii, *Quantum Electrodynamics* (Pergamon Press, Oxford, 1982).
[16] W. Becker, Laser Part. Beams **9**, 603 (1991).
[17] B. Richards and E. Wolf, Proc. R. Soc. A **253**, 358 (1959).
[18] J. J. Stamnes, *Waves in Focal Regions* (Adam Hilger, Bristol, 1986).
[19] R. Dorn, S. Quabis, and G. Leuchs, J. Mod. Opt. **50**, 1917 (2003).